

## Probing electron captures on $^{56}\text{Ni}$ : A new technique to extract Gamow-Teller strengths of unstable nuclei.

G. Perdikakis<sup>\*†1,2</sup>, M. Sasano<sup>1,2§</sup>, R. G. T. Zegers<sup>1,2,3</sup>, Sam M. Austin<sup>1,2</sup>, D. Bazin<sup>1</sup>, B. A. Brown<sup>1,2,3</sup>, C. Caesar<sup>4</sup>, A. L. Cole<sup>5</sup>, J. M. Deaven<sup>1,2,3</sup>, N. Ferrante<sup>6</sup>, C. J. Guess<sup>2,7</sup>, G. W. Hitt<sup>8</sup>, R. Meharchand<sup>1,2,3¶</sup>, F. Montes<sup>1,2</sup>, J. Palardy<sup>6</sup>, A. Prinke<sup>1,2,3</sup>, L. A. Riley<sup>6</sup>, H. Sakai<sup>9</sup>, M. Scott<sup>1,2,3</sup>, A. Stolz<sup>1</sup>, L. Valdez<sup>1,2,3</sup> and K. Yako<sup>10</sup>

<sup>1</sup> National Superconducting Cyclotron Laboratory, Michigan State University, East Lansing, Michigan 48824-1321, USA

<sup>2</sup> Joint Institute for Nuclear Astrophysics, Michigan State University, East Lansing, Michigan 48824, USA

<sup>3</sup> Department of Physics and Astronomy, Michigan State University, East Lansing, Michigan 48824, USA

<sup>4</sup> GSI Darmstadt, Helmholtz-Zentrum für Schwerionenforschung, D-64291 Darmstadt, Germany

<sup>5</sup> Physics Department, Kalamazoo College, Kalamazoo, Michigan 49006, USA

<sup>6</sup> Department of Physics and Astronomy, Ursinus College, Collegeville, Pennsylvania 19426, USA

<sup>7</sup> Department of Physics, University of Massachusetts Lowell, Lowell, Massachusetts 01854, USA

<sup>8</sup> Khalifa University of Science, Technology & Research, 127788 Abu Dhabi, UAE

<sup>9</sup> RIKEN Nishina Center, Wako 351-0198, Japan

<sup>10</sup> Department of Physics, University of Tokyo, Tokyo 113-0033, Japan

Electron captures on iron-group nuclei near  $^{56}\text{Ni}$  play an important role in the evolution of type Ia and type II supernovae. A new technique that allows the study of Gamow-Teller (GT) strengths from unstable nuclei has been developed at NSCL and used to probe the GT response of  $^{56}\text{Ni}$ . The  $^{56}\text{Ni}(p,n)^{56}\text{Cu}$  charge-exchange reaction at 110 MeV/u was employed to extract GT strengths from  $^{56}\text{Ni}$  for the first time. Because of isospin symmetry, the extracted strength distribution is also valid for the  $^{56}\text{Ni} \rightarrow ^{56}\text{Co}$  electron-capture direction, which is most important for astrophysical applications. The results were compared with shell-model theory employing two modern interactions, GXPF1A/J and KB3G. The calculation with the GXPF1A/J interaction provides a better match to the experimental results. Besides the results for  $^{56}\text{Ni}$ , newly extracted Gamow-Teller strengths from the  $^{55}\text{Co}(p,n)$  reaction are presented.

*XII International Symposium on Nuclei in the Cosmos,  
August 5-12, 2012  
Cairns, Australia*

\*Speaker.

†Email: [perdi1g@cmich.edu](mailto:perdi1g@cmich.edu)

‡Present address: Department of Physics, Central Michigan University, Mt. Pleasant, MI 48859, USA

§Present address: RIKEN Nishina Center, 2-1 Hirosawa, Wako, Saitama 351-0198, Japan

¶Present address: Los Alamos National Laboratory, Los Alamos, New Mexico 87545, USA

## 1. Introduction

Weak reaction rates, in particular electron capture rates, are a key ingredient of astrophysical simulations of thermonuclear and core-collapse supernovae. In Core collapse supernovae, when a massive star has gone through Si burning, the remaining iron-core is sustained against gravitational collapse by the degenerate electron pressure in the core. The electrons however get gradually captured by the iron-region nuclei in the core and the pressure drops [1]. Electron captures (EC) thus play a significant role in the dynamics of the collapse. Studies of properties like electron fraction, density, entropy, and other characteristics of the astrophysical environment that affect the pre-supernova phase, demonstrate that the use of different electron-capture rate inputs can have a significant effect [2].

In type Ia supernovae the nature of the progenitor system is still uncertain. Progenitor properties (e.g. age of stellar population) are related to the peak brightness of the event which can be measured by astronomical observation [3]. The observed peak brightness is correlated to the abundance of Ni produced [4]. Astrophysical simulations starting with different assumptions about the progenitor system result in varying abundances for Ni and other iron-region nuclei. Type Ia supernovae are thought to be responsible for more than 50% of the observed iron-group abundances in the solar system. Astrophysical models can be constrained if the uncertainties in the nuclear reaction rates, and the electron-capture rates in particular, are small [5].

Electron captures proceed through Gamow-Teller (GT) transitions. Charge-exchange reactions at intermediate energies have become the preferred tool to extract Gamow-Teller strength distributions, since direct measurements through  $\beta$  or EC-decay are only available for a very limited number of transitions. The extraction of GT strength from CE data is based on the well-known proportionality between the differential cross section at vanishing momentum transfer and GT strength. This proportionality was studied extensively in the late eighties for already the case of nucleon induced [(p,n) and (n,p)] reactions [6], and more recently for reactions induced by composite probes, such as (d, $^2\text{He}$ ), ( $^3\text{He}$ ,t) and (t, $^3\text{He}$ ). [7–9].

Simulations of supernovae have to include electron-capture rate input for a large number of nuclei. Typically spanning the region of  $40 \leq A \leq 120$ , the majority of the involved isotopes are unstable. In addition, due to the relatively high temperatures during the late evolution of the above-mentioned explosive scenario, the contribution of ECs on thermally excited states of the nuclei involved has to be taken into account. The experimental determination of all the participating rates, or even of a significant subset, is impossible. One has to resort to theoretical estimates to obtain reliable electron-capture rates over the range of nuclei involved. The theoretical models that are used to generate Gamow-Teller strength distributions have to be developed and tested on the basis of experimental data. Experiments should thus be focused on extracting GT strength distributions from nuclei that can provide detailed information about basic properties of the underlying theory. In addition, direct measurements for nuclei that are particularly abundant in the relevant stellar environments are important as well.

$^{56}\text{Ni}$  falls in both these categories. In the independent particle model,  $^{56}\text{Ni}$  with  $N = Z = 28$  is doubly magic. However, since both protons and neutrons occupy the same major (pf) shell, the proton-neutron interaction is relatively strong, thereby softening the  $f_{7/2}$  core [10, 11]. Shell-model calculations with the KB [12, 13] and GXPF1 [14–16] families of interactions both predict that

the probability of a closed  $f_{7/2}^{16}$  shell configuration for  $^{56}\text{Ni}$  is about 65%. GT strengths calculated with the KB family of interactions, which have been used in the generation of a weak-reaction rate library for astrophysical calculations [17], differ drastically [16] from those using the GXPF1 family. The differences between the two sets of calculations impact the estimates for EC rates on  $^{56}\text{Ni}$  by as much as 30% [16]. Moreover, by resolving the ambiguity between the two shell-model calculations for the case of  $^{56}\text{Ni}$ , it becomes possible to improve the EC rate estimates for many nuclei in the iron group, which leads to an overall improvement of the input for the astrophysical simulations. A benchmark of this approach is the GT strength from  $^{55}\text{Co}$ , a nearby odd-A, odd-Z nucleus of astrophysical interest which was also studied in this work.

A new technique for measuring the (p,n) CE reaction at  $\sim 110$  MeV/u in inverse kinematics has been used in this work to determine the GT strengths from  $^{56}\text{Ni}$  and  $^{55}\text{Co}$  [18, 19]. The method relies on measuring the energy and laboratory scattering angle of the recoiling neutron, from which the excitation energy of the residual nucleus and center-of-mass scattering angle are determined. The residual nucleus or one of its decay products (if the excitation energy exceeds the threshold for particle decay) is also detected for unambiguous assignment of the reaction channel. The technique is suitable for experiments with unstable isotopes of any mass, up to high excitation energies and signifies a new experimental capability to routinely study CE reactions with unstable nuclei.

A detector that can measure neutrons of relatively low energy ( $\sim 200$  keV and above) with good energy and angle resolutions and with high efficiencies is required. With those goals, the Low Energy Neutron Detector Array (LENDa) has been developed at NSCL [20]. LENDa is composed of 24 neutron detectors and provides fast timing ( $\sim 400$  ps timing resolution), reasonable position resolution ( $\sim 6$  cm) and a low neutron energy detection threshold of 150 keV. In the following, details of the  $^{56}\text{Ni}$  and  $^{55}\text{Co}(p,n)$  experiments will be presented. These will be followed by the results from the analysis of the experimental data and a comparison with suitable theoretical calculations.

## Experimental

A beam of  $^{58}\text{Ni}$  at 160 MeV/u from the NSCL Coupled Cyclotron Facility was fragmented on a  $410$  mg/cm<sup>2</sup> thick Be production target at the entrance of the A1900 fragment separator. A  $237$ -mg/cm<sup>2</sup> thick aluminum wedge was placed at the intermediate image of the A1900. Contaminant species were mostly removed by a momentum-defining slit at the exit of the A1900. The resulting cocktail beam had a momentum spread of  $\pm 0.25\%$ , and an intensity of  $8 \times 10^5$  particles per second. It was composed by  $^{56}\text{Ni}$  (66%) at 110 MeV/u,  $^{55}\text{Co}$  at 106 MeV/u (32%), and  $^{54}\text{Fe}$  at 102 MeV/u (2%). Beam particles were identified on an event-by-event basis by measuring the particles' timing relative to the cyclotron RF with a  $1\text{-cm}^2$  in-beam diamond detector [21] installed at the object of the S800 spectrograph [22].

The reaction target consisted of a liquid hydrogen cell, with an average thickness of  $60$  mg/cm<sup>2</sup> and a diameter of 35 mm. The hydrogen, kept at a pressure just above 1 atm and a temperature of about 19 K, was contained by  $125\text{-}\mu\text{m}$ -thick Kapton foils. The target was placed 65 cm upstream of the pivot point of the S800 spectrograph. A few runs with an empty target cell were acquired to estimate the background due to events originated from the Kapton foils.

The liquid hydrogen target was surrounded by the newly-constructed Low Energy Neutron Detector Array (LENDa) [20] which registered the timing of a neutron hit relative to the signal from

an in-beam diamond detector at the object of the spectrometer [16], the corresponding scintillation light output, and the neutron's hit position. This information provided the neutron emission angle and energy on an event-by-event basis. For the experiment, 12 bars were placed to the left and 12 to the right of the beam line covering laboratory angles between  $20^\circ$  and  $70^\circ$ . The total solid angle coverage by LENDA was 0.32 sr.

Event-by-event particle identification (PID) for beam residues produced in the target was performed in the S800 spectrometer [22]. The energy loss ( $\Delta E$ ) and time of flight (TOF) of the residues were measured with an ionization chamber and a plastic scintillator, respectively, which were located in the focal plane of the spectrograph. The reference for the TOF measurement was provided by the signal from the above-mentioned diamond detector. Two cathode-readout drift chambers (CRDCs) at the focal plane provided two-dimensional hit-position information, which was used to determine the momentum and angle of each particle track.

## Analysis

The PID information taken from the focal plane of S800 in coincidence with neutron events was used to identify the reaction products and the various background contributions. For the  $^{56}\text{Ni}$  component of the incoming beam the relevant PID spectrum is presented in figure 1. The  $^{56}\text{Cu}$ ,  $^{55}\text{Ni}$ , and  $^{54}\text{Co}$  loci in the figure correspond to possible final products of the  $^{56}\text{Ni} + p$  reaction. For excitation energies below the proton separation energy,  $^{56}\text{Cu}$  is the only product of the  $^{56}\text{Ni}(p,n)$  reaction. Above the one proton separation threshold,  $^{56}\text{Cu}$  can decay to  $^{55}\text{Ni}$ , and above the two proton separation energy,  $^{54}\text{Co}$  can be the final product. The corresponding neutron spectra for these 3 cases are shown in figure 2. The lines in the spectra correspond to the neutron kinematics for states in  $^{56}\text{Cu}$ . The fourth spectrum of the figure, gated on  $^{53}\text{Co}$ , shows no correlation to the (p,n) reaction and corresponds to accidental coincidences between background neutrons (most probably from knockout reactions) and the S800 focal plane. The largest source of background was caused by neutron-knockout events, in which a fast neutron was scattered of surrounding material back into LENDA. Other contributions to the background, such as the interaction with the target cell materials and random coincidences, were less significant.

## Results

The results for the Gamow-Teller strength from  $^{56}\text{Ni}$  and  $^{55}\text{Co}$  that were deduced in this work are presented in figure 3. The results of shell model calculations using the GXPF1A [15] or GXPF1J [16] effective interactions of the GXPF1 [14] family and the KB3G [13] effective interaction of the KB family are presented in the same figure. All calculations in figure 3 were smeared with the resolution of the experimental data in order to compare with the measurements. A quenching factor of  $(0.74)^2$  was used to account for the overestimation of the theoretical strength due to missing degrees of freedom in the shell-model calculations [23]. The calculations with the KB3G interaction feature a single maximum in the strength distribution for both  $^{56}\text{Ni}$  and  $^{55}\text{Co}$  cases. This strength appears lower in excitation energy and is more concentrated compared to the experimental data. In the case of  $^{56}\text{Ni}$ , the double-peak structure observed in the experiments is missed. The GXPF1 family of interactions shows a better agreement with the data for both nuclei. For the

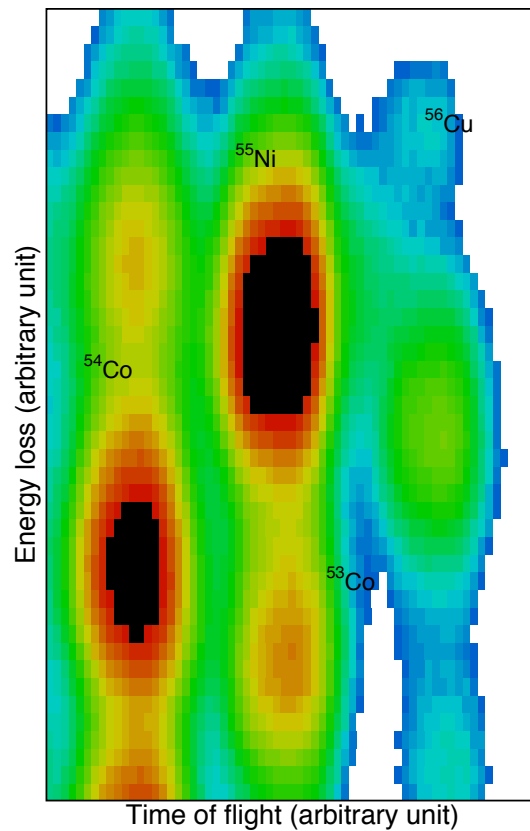


Figure 1: Particle identification plot of Energy loss versus TOF for the reaction products detected at the focal plane of S800 in coincidence with neutrons in LENDA.

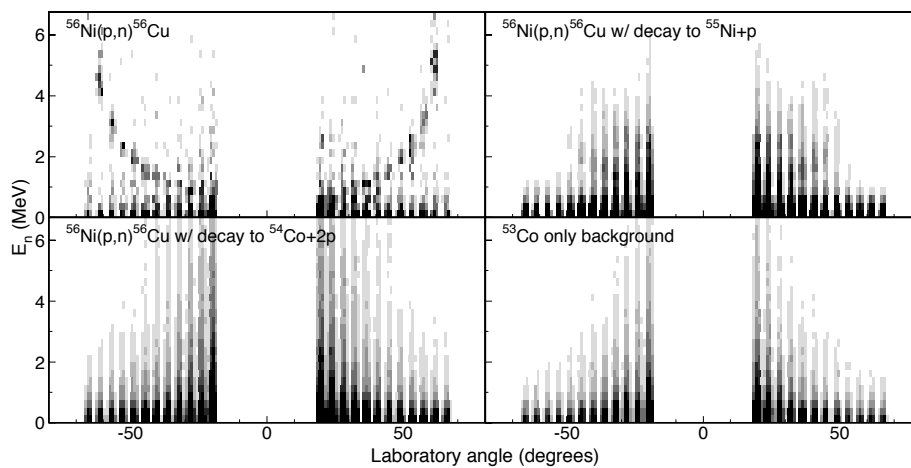


Figure 2: Experimental spectra of the neutron events in LENDA, gated with events on different PID loci. In the panels associated with final states in which  $^{56}\text{Cu}$ ,  $^{55}\text{Ni}$  and  $^{54}\text{Co}$  were detected in the spectrometer, kinematic correlations associated with (p,n) reactions can be observed. For the case where  $^{53}\text{Co}$  is observed, only background is present.

case of  $^{56}\text{Ni}$  it reproduces the basic characteristics of the double-peaked strength distribution. The two interactions of this family, GXPF1A and GXPF1J represent successive improvements of the GXPF1 interaction constrained by data [15, 16] for nuclei in the pf-shell and thus feature slight differences in the calculated strength distribution for  $^{56}\text{Ni}$  as seen in a comparison between figures 3 a) and 3 c). Since the most sophisticated database of weak reaction rates [17] is based on calcu-

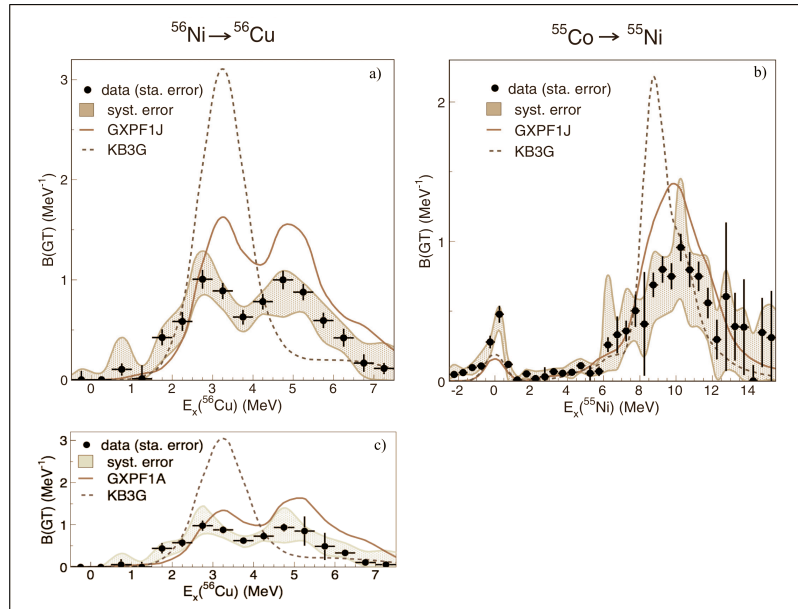


Figure 3: Experimental results for the Gamow-Teller strength. The experimental data points are represented by black bullets. The green area surrounding the data corresponds to the estimated systematic uncertainty while the error bars correspond to the statistical uncertainty of the data. The blue dashed line corresponds to shell model calculations using the KB3G effective interaction [13] while the red line corresponds to calculations using the GXPF1 interaction [14]. a) Experimental data and theoretical calculations with KB3G and GXPF1J interactions for the GT strength from  $^{56}\text{Ni}$  through the reaction  $^{56}\text{Ni}(p,n)$ . b) The same for the GT strength from  $^{55}\text{Co}$  through the reaction  $^{55}\text{Co}(p,n)$ . c) Same as a) but using GXPF1A interaction.

lations with an interaction from the KB family of interaction, it appears that further improvement can still be made on the basis of the present results.

## Conclusions

The GT strength from the astrophysically important nuclei  $^{56}\text{Ni}$  and  $^{55}\text{Co}$  has been measured for the first time using a novel technique that enables the study of CE reactions on unstable nuclei without any limitations in mass or energy range. The results have been used to test shell-model effective interactions. It is found that modest improvements to the most modern library of weak rates are feasible by employing an interaction from the GXPF1 family of interactions, rather than from the KB3G family.

## Acknowledgments

This work was supported by the US NSF [PHY-0822648 (JINA), PHY-0606007, PHY-0758099, and PHY-1068217], the US Department of Energy (DE-FG02-94ER40848), and the Research Corporation for Science Advancement.

## References

- [1] S. Woosley and H. Th. Janka. The physics of core collapse supernovae. *arXiv:astro-ph/*, (0601261v1), 2006.
- [2] W. R. Hix, O. E. B. Messer, A. Mezzacappa, M. Liebendörfer, J. Sampaio, K. Langanke, D. J. Dean, and G. Martínez-Pinedo. Consequences of nuclear electron capture in core collapse supernovae. *Phys. Rev. Lett.*, 91:201102, Nov 2003.
- [3] Brendan K. Krueger, Aaron P. Jackson, Dean M. Townsley, Alan C. Calder, Edward F. Brown, and F. X. Timmes. On variations of the brightness of type ia supernovae with the age of the host stellar population. *arXiv: astro-ph*, (1007.0910v1), 2010.
- [4] F. Brachwitz, D. J. Dean, W. R. Hix, K. Iwamoto, K. Langanke, G. Martínez-Pinedo, K. Nomoto, M. R. Strayer, F.-K. Thielemann, and H. Umeda. The role of electron captures in chandrasekhar-mass models for type ia supernovae. *The Astrophysical Journal*, 536(2):934, 2000.
- [5] K. Iwamoto, F. Brachwitz, K. Nomoto, N. Kishimoto, H. Umeda, W. R. Hix, and F.-K. Thielemann. Nucleosynthesis in chandrasekhar mass models for type ia supernovae and constraints on progenitor systems and burning-front propagation. *The Astrophysical Journal Supplement Series*, 125(2):439, 1999.
- [6] T. N. Tadeucci. The (p,n) reaction as a probe of beta decay strength. *Nuclear Physics A*, 469:125, 1987.
- [7] E. W. Grewe, C. Bäumer, A. M. van den Berg, N. Blasi, B. Davids, D. De Frenne, D. Frekers, P. Haefner, M. N. Harakeh, M. Huynyadi, E. Jacobs, B. Junk, A. Korff, A. Negret, P. von Neumann-Cosel, L. Popescu, S. Rakers, and H. J. Wörtche. Gamow-teller transitions to  $^{32}\text{P}$  studied through the  $^{32}\text{S}(d,^2\text{He})$  reaction at  $E_d = 170$  MeV. *Phys. Rev. C*, 69:064325, Jun 2004.
- [8] R. G. T. Zegers et al. Extraction of weak transition strengths via the ( $^3\text{He}, t$ ) reaction at 420 mev. *Phys. Rev. Lett.*, 99:202501, Nov 2007.
- [9] G. Perdikakis et al. Gamow-Teller unit cross sections for ( $t, ^3\text{He}$ ) and ( $^3\text{He}, t$ ) reactions. *Phys. Rev. C*, 83:054614, May 2011.
- [10] K. Minamisono, P. F. Mantica, T. J. Mertzimekis, A. D. Davies, M. Hass, J. Pereira, J. S. Pinter, W. F. Rogers, J. B. Stoker, B. E. Tomlin, and R. R. Weerasiri. Nuclear magnetic moment of the  $^{57}\text{Cu}$  ground state. *Phys. Rev. Lett.*, 96:102501, Mar 2006.
- [11] A. F. Lisetskiy, N. Pietralla, M. Honma, A. Schmidt, I. Schneider, A. Gade, P. von Brentano, T. Otsuka, T. Mizusaki, and B. A. Brown. Experimental evidence for  $^{56}\text{Ni}$ -core breaking from the low-spin structure of the  $N = Z$  nucleus  $^{58}_{29}\text{Cu}_{29}$ . *Phys. Rev. C*, 68:034316, Sep 2003.
- [12] E. Caurier, F. Nowacki, A. Poves, and J. Retamosa. Shell model study of the neutrinoless double beta decays. *Nuclear Physics A*, 654(1, Supplement 1):973c – 976c, 1999.
- [13] A. Poves, J. Sánchez-Solano, E. Caurier, and F. Nowacki. Shell model study of the isobaric chains  $A=50$ ,  $A=51$  and  $A=52$ . *Nuclear Physics A*, 694(1–2):157 – 198, 2001.

- [14] M. Honma, T. Otsuka, B. A. Brown, and T. Mizusaki. New effective interaction for  $pf$ -shell nuclei and its implications for the stability of the  $N = Z = 28$  closed core. *Phys. Rev. C*, 69:034335, Mar 2004.
- [15] M Honma, T Otsuka, T Mizusaki, M Hjorth-Jensen, and B A Brown. Effective interaction for nuclei of  $A = 50$ – $100$  and gamow–teller properties. *Journal of Physics: Conference Series*, 20(1):7, 2005.
- [16] Toshio Suzuki, Michio Honma, H el ene Mao, Takaharu Otsuka, and Toshitaka Kajino. Evaluation of electron capture reaction rates in Ni isotopes in stellar environments. *Phys. Rev. C*, 83:044619, Apr 2011.
- [17] K. Langanke and G. Mart ınez-Pinedo. Rate tables for the weak processes of  $pf$ -shell nuclei in stellar environments. *Atomic Data and Nuclear Data Tables*, 79(1):1 – 46, 2001.
- [18] M. Sasano, G. Perdikakis, R. G. T. Zegers, Sam M. Austin, D. Bazin, B. A. Brown, C. Caesar, A. L. Cole, J. M. Deaven, N. Ferrante, C. J. Guess, G. W. Hitt, R. Meharchand, F. Montes, J. Palardy, A. Prinke, L. A. Riley, H. Sakai, M. Scott, A. Stolz, L. Valdez, and K. Yako. Gamow-Teller transition strengths from  $^{56}\text{Ni}$ . *Phys. Rev. Lett.*, 107:202501, Nov 2011.
- [19] M. Sasano, G. Perdikakis, R. G. T. Zegers, Sam M. Austin, D. Bazin, B. A. Brown, C. Caesar, A. L. Cole, J. M. Deaven, N. Ferrante, C. J. Guess, G. W. Hitt, M. Honma, R. Meharchand, F. Montes, J. Palardy, A. Prinke, L. A. Riley, H. Sakai, M. Scott, A. Stolz, T. Suzuki, L. Valdez, and K. Yako. Extraction of Gamow-Teller strength distributions from  $^{56}\text{Ni}$  and  $^{55}\text{Co}$  via the  $(p, n)$  reaction in inverse kinematics. *Phys. Rev. C*, 86:034324, Sep 2012.
- [20] G. Perdikakis et al. LENDA: A low energy neutron detector array for experiments with radioactive beams in inverse kinematics. *Nucl. Instr. Meth. Phys. Res. A*, 686(0):117 – 124, 2012.
- [21] A. Stolz, M. Behravan, M. Regmi, and B. Golding. Heteroepitaxial diamond detectors for heavy ion beam tracking. *Diamond and Related Materials*, 15(4–8):807 – 810, 2006.
- [22] D. Bazin, J. A. Caggiano, B. M. Sherrill, J. Yurkon, and A. Zeller. The S800 spectrograph. *Nucl. Instr. Methods B*, 204:629 – 633, 14th International Conference on Electromagnetic Isotope Separators and Techniques Related to their Applications 2003.
- [23] G. Mart ınez-Pinedo, A. Poves, E. Caurier, and A. P. Zuker. Effective  $g_A$  in the  $pf$  shell. *Phys. Rev. C*, 53:R2602–R2605, Jun 1996.